J. Membrane Biol. 43, 295–315 (1978)

Action of Extracellular pH on Na^+ and K^+ Membrane Currents in the Giant Axon of *Loligo Vulgaris*

E. Carbone, R. Fioravanti, G. Prestipino, and E. Wanke

Laboratorio di Cibernetica e Biofisica, Consiglio Nazionale delle Ricerche, 16032 Camogli, Italy

Received 14 March 1978

Summary. Voltage-clamp currents and resting membrane potential of squid giant axons have been studied at extracellular pH varying between 4 and 10. The membrane currents, analyzed according to the Hodgkin-Huxley equations, showed that sodium permeability, $P_{Na}(E)$, and potassium conductance, $g_K(E)$, curves were shifted toward positive voltages by different amounts and slightly depressed as the external pH was lowered. Under the same conditions, $\tau_m(E)$ and $\tau_n(E)$ were found to be enhanced and shifted to a larger extent in the same direction. The rate constants α_m and α_n were shifted substantially toward positive voltages, but β_m and β_n changed hardly at all. The shift of the $\alpha_m(E)$ curve was analyzed in terms of a fixed surface charge model; it indicates that unspecific negative groups with an approximate pK_a of 4.5 are located in the vicinity of sodium active sites with an average charge separation of 8 Å. A similar figure is obtained for the potassium system from the shift of the $\alpha_n(E)$ curve.

The effects of external pH on the mechanisms of ionic conductance changes have been recently investigated in different nerve preparations (Hille, 1968; Mozhayeva & Naumov, 1970; Shrager, 1974; Schauf & Davis, 1976). By increasing the external hydrogen ion concentration in voltage clamped nerves, both peak sodium and the late steady-state currents were reported to be reversibly slowed and depressed proportionally to the pH value. Depending upon the nerve preparation, the kinetics and the maximum values of sodium and potassium conductance were found to have different behaviors, reflecting substantial differences from membrane to membrane. However, all the data were found more or less consistent with the idea that the voltage shift in the parameters governing the time course of membrane current was the result of protons binding to fixed negative surface charges. The reduction in conductances was explained by a specific block of the ionic channels by hydrogen ions. Furthermore, Woodhull (1973) found evidence in the frog node for a voltage-dependent block of Na^+ channels.

0022-2631/78/0043-0295 $04.20
© Springer-Verlag New York Inc. 1978

For the squid axon no extensive studies have been reported, so far. Early investigations on the effects of different electrophysiological conditions upon the cytoplasmic pH mainly concerned the question of whether the hydrogen ion distribution across the membrane could be regulated by a Donnan equilibrium, and little attention was devoted to the changes in the ionic conductance mechanism evoked by lowering the external pH (Caldwell, 1958; Spyropoulos, 1960; Bicher & Ohki, 1972). The voltage clamp data available (Ehrenstein & Fishman, 1971; Stillman, Gilbert & Lipicky, 1971) do not report any quantitative result for the potassium system, and they are not suitable for a detailed analysis of the Na^+ conductance.

The present paper reports a more complete series of experiments on voltage-clamp currents and resting potential of squid axons bathed in solutions whose pH ranged between 10 and 4. Data analysis, carried out on the basis of the Hodgkin and Huxley (1952*b*) theory, indicates that external hydrogen ions produce a different voltage shift of the forward and backward reaction rate constants of both sodium and potassium systems. The results for the potassium system are consistent with those reported by Shrager (1974) on crayfish axons. For the Na^+ channels the analysis indicates that m and h are influenced by the external hydrogen ion concentration in a different way and that, at acid pH the maximum sodium permeability is reduced.

Materials and Methods

Experimental Procedure and Measuring System

Giant axons of 500–700 μm diameter were isolated from the mantle of the squid *Loligo vulgaris*, available in Camogli (Italy), following the procedure of Conti, De Felice and Wanke (1975). All experiments were carried out with fibers carefully cleaned of the connective tissues and mounted on a Lucite chamber similar to that described by Conti *et al.* (1975). Twenty-six millimeters of axon were bathed in the external medium, while a central zone of 18 mm length was space clamped using a "piggy-back" internal electrode (Chandler & Meves, 1965) inserted longitudinally through a cut at one end of the fiber.

The internal electrode consisted of a 50 to 70-μm glass pipette glued together with a 75-μm Pt wire by means of an extremely thin layer of sticky-wax. The platinum wire was used as current electrode and platinized for a length of 22 mm symmetrically to the tip of the glass capillary, while the remaining part was electrically insulated with a thin dry layer of *formvar*. The glass pipette served to record the internal potential and contained 535 mM KCl. To reduce its high frequency impedance, a 20-μm floating Pt wire was inserted inside the pipette. An agar-agar bridge ensured the electrical continuity between the KCl solution and a silver-silver chloride cell. The external current electrode was a double foil of Pt black ($18 \times 4\,mm^2$) placed longitudinally on each side of the axon;

grounded guard electrodes ($4 \times 4\,mm^2$ Pt black foils) were placed on both sides of the central region. Positive feedback was used to compensate as far as possible (90%) for the effects of the resistance in series with the axon membrane ($4\Omega \cdot cm^2$). No corrections for the electrode junction potentials (Cole & Moore, 1960) were made.

Normally, current records at different voltage clamp steps were obtained starting from a holding potential, E_h, of -80 mV. The duration of the pulse varied, ranging from 20 msec (pH 8) to 40 or 90 msec at low pH. At the end of each run a hyperpolarizing pulse of 50 mV amplitude was delivered from E_h to determine the time course of the leakage current. The resting potential was also checked at the beginning and at the end of each run.

Data acquisition was performed by sampling the time course of the membrane current with 1000 points at intervals of 20, 40, or 100 μsec, using an averaging computer (HP 4580 B) employed as an analog to digital converter. The digital record was subsequently read-out at slower rate and stored on tape with a FM recorder (HP 3960). The data were then analyzed by a DECLAB computer (Digital Equipment Corp.).

Solutions

All the control experiments were done with axons bathed in artificial sea water (ASW) having the following composition (mM): NaCl, 450; KCl, 10; $CaCl_2$, 15; $MgCl_2$, 50; pH adjusted to 8 by adding 2 mM Tris-HCl. Test solutions with pH above and below 8 were prepared by replacing 20 mM NaCl with an equal amount of buffering solutions. Lower concentrations of buffer were found to increase the time required by the axonal membrane to reach a steady level of electrophysiological conditions, while higher amounts were found to be no more effective than 20 mM. A series of buffers employed in these experiments included: Na-phthalate (pH range: 4–5.5), Tris-maleate (5.3–6.7), Na-phosphate (6.3–7.7), Tris-HCl (7.3–8.7) and Na-borate (8.3–10).

To rule out any possible error due to residual amounts of the exchanged solutions, in few axons the pH of the external bath was measured at the end of the experiment and found to lie within ± 0.05 pH units of the initial value. In most of the experiments the temperature of the bath was maintained between 2 and 4 °C with an accuracy of 0.1 °C. When required, 10^{-7} M of tetrodotoxin (TTX) were added to the external solution.

Data Analysis

The time course of the current flowing across the membrane during a voltage clamp pulse was analyzed according to the Hodgkin-Huxley model (1952*b*). The parameters m_∞, n_∞, τ_m, τ_n and τ_h were obtained directly from the fit of the current records assuming $m_\infty(E_h) = n_\infty(E_h) = h_\infty(E) = 0$, and $h_\infty(E_h) = 1$ (E_h being the initial and E the final potential). The constants of the system were found to have the following values: $\bar{P}_{Na} = 1.4\text{–}1.5 \times 10^{-4}\,cm \cdot sec^{-1}$, $\bar{g}_K = 40 - 55\,mS \cdot cm^{-2}$, and $g_e = 0.3 - 0.5\,mS \cdot cm^{-2}$. The equilibrium potentials were determined for sodium (E_{Na}) following the HH procedure (Hodgkin & Huxley, 1952*a*); for potassium, after extrapolation at time zero of $E_K(t)$ values obtained according to the method of Adelman, Palti & Senft, 1973; for leakage, (E_1) after extrapolation at $I = 0$ of the steady-state $I - E$ relation measured at large hyperpolarizing voltages (-110, -90 mV).

The rectification of the sodium channel (Conti, Fioravanti & Wanke, 1973; Keynes & Rojas, 1976) was accounted for by using the constant field equation (Goldman, 1943; Hodgkin & Katz, 1949), as done in the node of Ranvier by Dodge and Frankenhaeuser (1959).

In order to determine the exact time course of potassium conductance, the delayed currents were corrected for the changes of the K^+ equilibrium potential, $E_K(t)$, due to the increment in potassium concentration, $[K_e(t)]$ (Mole $\cdot$ cm^{-3}), in the periaxonal space. The model used is similar to that proposed by Frankenhaeuser and Hodgkin (1956), which assumes the existence of a thin outer layer with permeability to potassium ions P (cm $\cdot$ sec^{-1}), separated from the axonal membrane by a phenomenological aqueous space of thickness θ (cm). Under these conditions $[K_e(t)]$ will be governed by:

$$\theta \frac{d[K_e(t)]}{dt} = \frac{I_K(t)}{F} - P[K_e(t)], \tag{1}$$

where F is the Faraday constant and $I_K(t)$ is the recorded potassium current. A negative term taking into account the flow of K^+ ions due to the electric potential gradient existing across the diffusion layer should be added to the right-hand side of Eq. (1) (Adelman *et al.*, 1973). Omission of this term introduces an error in the computation of the outward diffusion of potassium ions, which can be estimated to be, at worst, 15% of the total flow (Adams, 1973).

Assuming $I_K(t)$ to be an exponential function to the fourth power and I_∞ its steady limiting value, the solution of Eq. (1) is given by:

$$[K_e(t)] = \frac{I_\infty}{F\theta} \sum_{j=0}^{4} (-1)^j \binom{4}{j} \frac{e^{-jt/\tau_n} - e^{-Pt/\theta}}{P/\theta - j/\tau_n}. \tag{2}$$

I_∞ and τ_n were obtained directly from the fit of the current density records, while P and θ were determined one single time for *Loligo vulgaris* from axons bathed in TTX-artificial sea water according to the following procedure. The time course of $g_K(t)$ was measured by evaluating the amplitude of the tail current at different times, following brief interruptions of a long voltage clamp step (Conti & Wanke, 1975). The measurements were repeated for several potentials at pH 8 and 5.2 and fitted with Eq. (2), together with:

$$g_K(t) = \frac{I_K(t)}{E - (RT/F) \ln \{([K]_0 + [K_e(t)])/[K]_i\}}, \tag{3}$$

$[K]_0$ and $[K]_i$ being the extra- and intracellular potassium ion concentration at rest. The pair of P and θ values yielding the best approximation were 2.3×10^{-4} cm $\cdot$ sec^{-1} and 100 Å, respectively.

Within the experimental error (15%), it was noticed that the corrected g_K curves could be fitted by $g_K = n^\gamma \bar{g}_K$ with $\gamma = 4$ only at low depolarizations. As the depolarizing step was increased, the exponent of n was found to decrease. This aspect of the problem, which involves a nontrivial modification of the concept of K^+ channel, requires more extended investigation in order to be properly treated. For this reason an attempt was made to fit $g_K(t)$ at different potentials with a constant exponent of n, it being found that $\gamma = 2$ was a reasonable choice.

Results

Effects of External pH on Membrane Currents

Figure 1 shows typical records of the ionic current density during voltage clamps at normal and low pH. The records were obtained starting from holding potential of -80 mV (E_h) at pH 8 and from

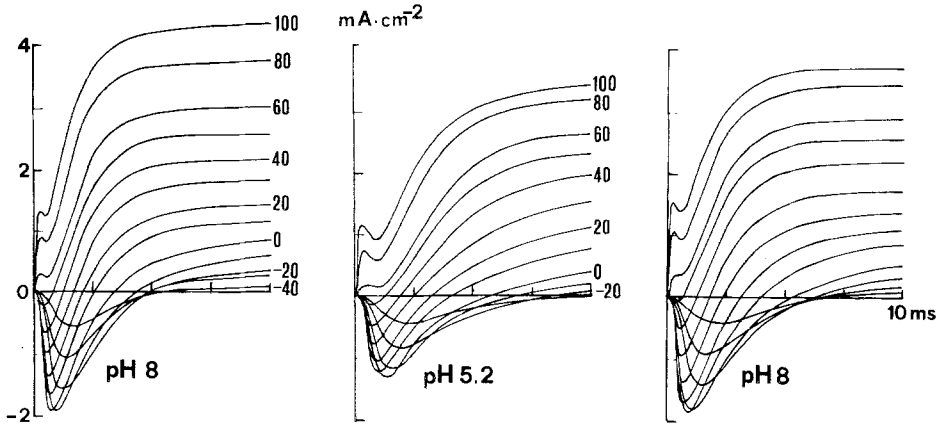

Fig. 1. Records of voltage clamp currents. Depolarizations to levels are indicated on the right of each record in mV. *Left:* axon in ASW, pH 8, $E_h = -80$ mV. *Center:* axon in ASW, pH 5.2, $E_h = -70$ mV. *Right:* recovery in ASW, pH 8. Records are corrected for leakage and capacity transient; temperature, 2 °C

-70 mV at low pH. In general, holding potentials varied from -90 to -60 mV, depending on the acidic conditions of the bath. This was suggested by independent measurements of the inactivation parameter h as a function of potential (*see* below) and by the observation that sustained hyperpolarizations progressively change the physiological conditions of the fiber at low pH. Depolarizing test pulses from the holding potential lasted long enough (20 to 90 msec) to allow the complete measurement of the late currents and terminated with a 40-mV brief repolarization to determine the instantaneous g_K. The short clamps (20 msec) were used for control experiments and large depolarizations, the long ones (90 msec) for low pH and small depolarizations.

Comparing traces at the same potential at normal and low pH shows: (i) a consistent increase in the time to peak of sodium inward currents, (ii) a large increase in the time to half-maximum steady-state currents, (iii) an amplitude reduction of both peak I_{Na} and steady-state I_K. From the figure it can also be argued that the effects of external pH on various current components are qualitatively different. At low pH and large depolarizations potassium currents are seen to be slowed down more than sodium currents in such a way that a clear temporal separation of the two current components can be observed. Similar findings were also reported by Shrager (1974) for crayfish axons.

In Fig. 2 the normalized magnitude of peak inward currents is plotted against voltage. Three important features are shown in the figure: (i) the maximum of peak currents is seen to decrease and shift monotonically

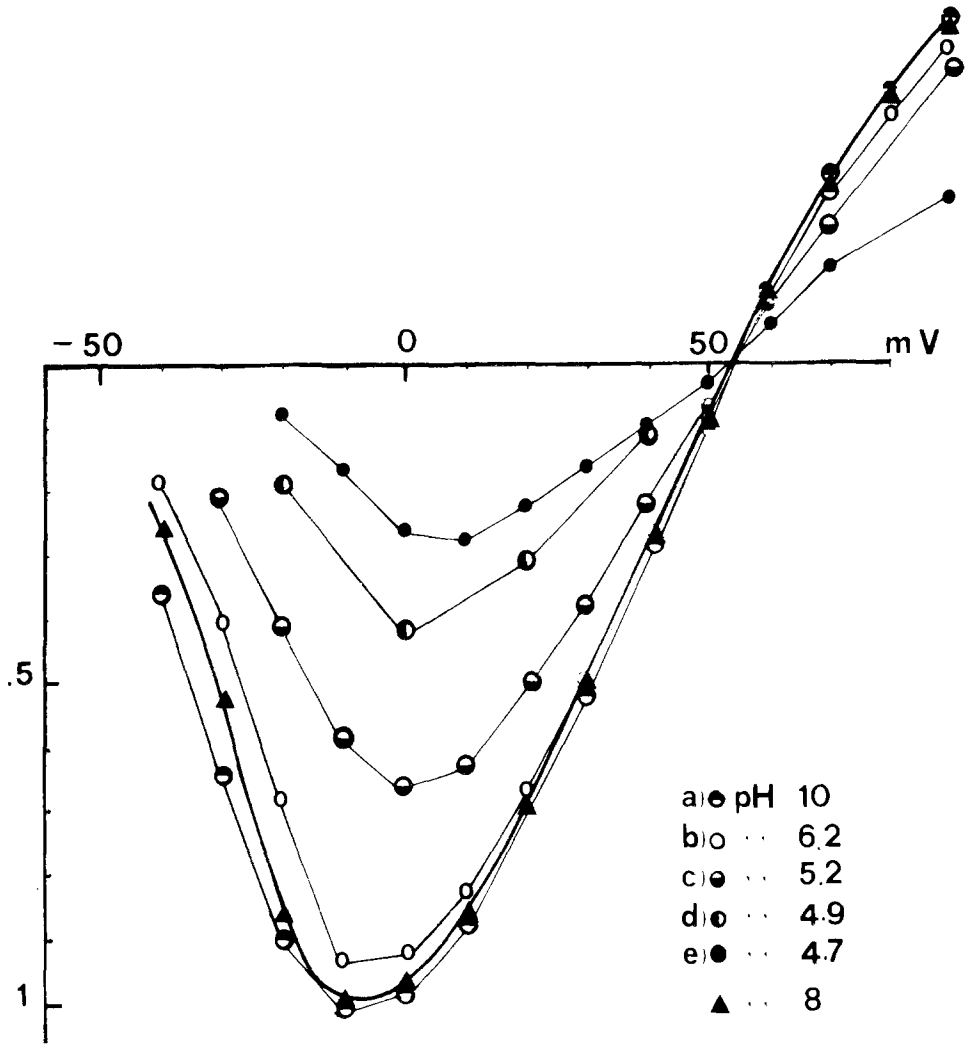

Fig. 2. Normalized peak inward current *vs.* membrane potential at different extracellular pH. Filled triangles represent the result of averaging the normalized peak transients of control measurements at pH 8. Data are corrected for leakage. Buffers employed, holding potentials, and temperature were: (*a*) Na-borate, −90 mV, 2 °C; (*b*) Tris-maleate, −80 mV, 2.5 °C; (*c*) Na-phthalate, −70 mV, 1.7 °C; (*d*) Na-phthalate, −70 mV, 3 °C; (*e*) Na-phthalate, −60 mV, 1.8 °C

toward more positive voltages with increasing acidity of the bath, as observed in other preparations (Hille, 1968; Drouin & Neumcke, 1974; Schauf & Davis, 1976). (ii) Both inward and outward sodium currents are similarly influenced by the external pH. (iii) The sodium reversal potential is not changed appreciably by varying the pH above 4.7, suggesting that external pH does not alter the ionic selectivity of sodium channels.

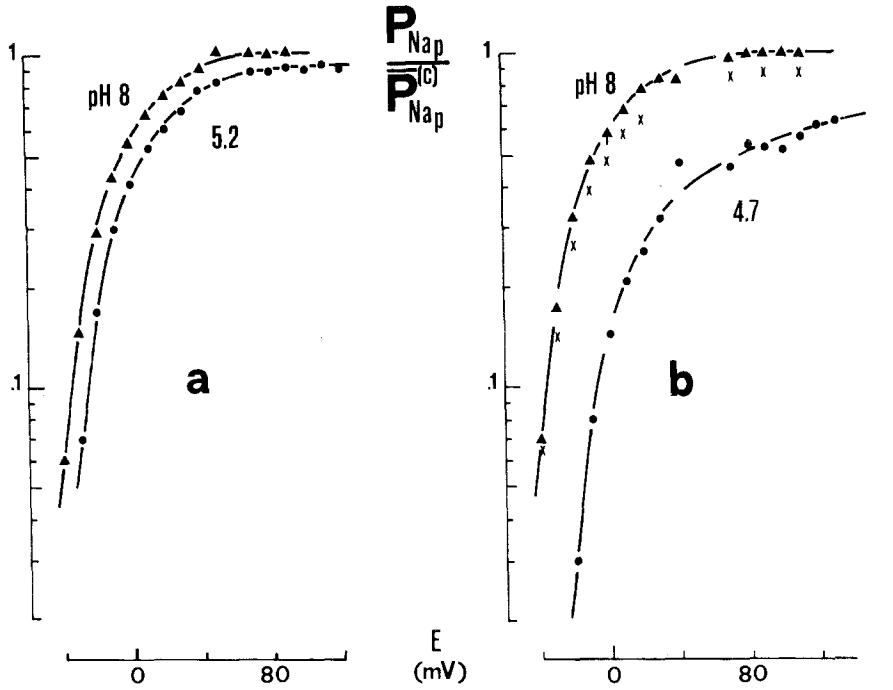

Fig. 3. (*a*)–(*b*): Sodium permeability at the peak of inward current, P_{Na_p}, normalized to the maximum value $\bar{P}^{(c)}_{Na_p}$ at pH 8. Data obtained from two different axons. The crosses correspond to the recovery at pH 8. $E_h = -80$ mV (pH 8); $E_h = -70$ mV (pH 5.2); $E_h = -60$ mV (pH 4.7); temperature, 2 °C. (*c*)–(*d*): Sodium permeability, P_{Na}, normalized to the maximum permeability $\bar{P}^{(c)}_{Na}$ at pH 8. The bars indicate the maximum error for an acceptable fit. The triangles and dots correspond to the above-peak permeabilities, converted to steady-state quantities according to Eq. (4). The curves at pH 8 were drawn by eye to best fit triangles and bars. Those at low pH are curves of the same shape but lower magnitude, which have been shifted toward positive potentials to best fit dots and bars

Figure 3a–b show the effects of external pH on sodium permeability at the peak of inward current. Data in *a* are taken from the current records of Fig. 1. Results in *b* are from an axon bathed in ASW, pH 4.7, which had a recovery within an acceptable range (crosses). The common aspect of Fig. 3*a–b* is a shift of $P_{Na_p}(E)$ toward more positive potentials and a reduction of the maximum peak permeability.

The effects of external pH on K currents are illustrated in Fig. 4. On the left are shown current density records obtained from TTX-treated axons at pH 8 (bottom) and 5.2 (top). On the right are plotted the instantaneous g_K values as a function of voltage, determined after a brief 40-mV repolarization at the end of the depolarizing pulse, according to the method of Adelman *et al.* (1973) and Conti and Wanke (1975). As for

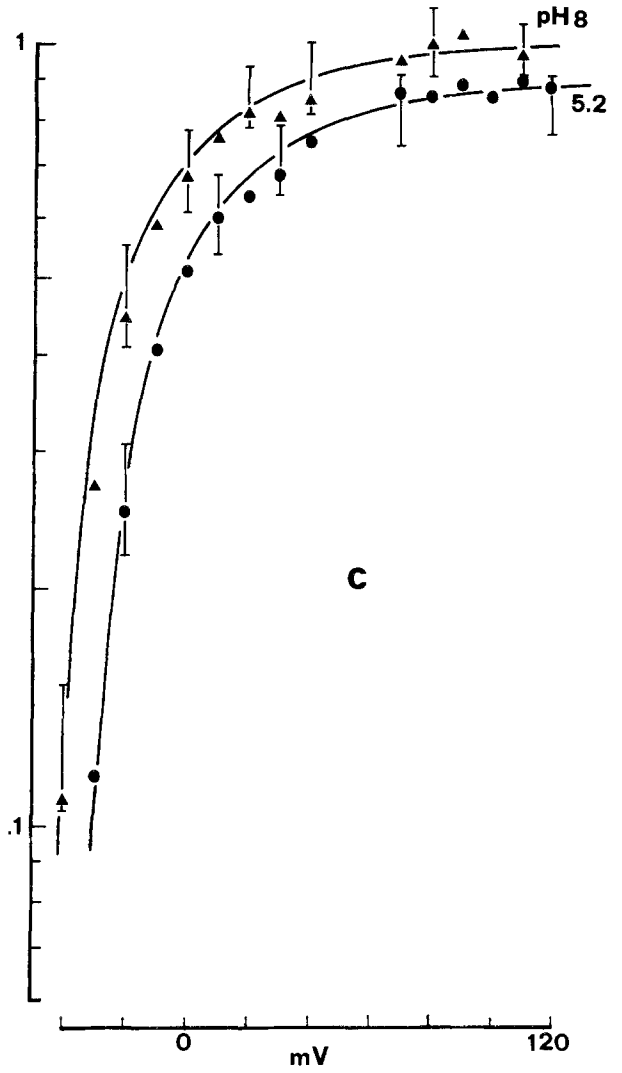

Fig. 3c

Na currents, increasing acidity causes an increase of the time to half-maximum steady-state current and a shift toward more positive potentials of the $g_K(E)$ characteristic.

Effects on Inactivation in the Steady State

Figure 5 shows the effects of external pH on the steady-state inactivation parameter $h(E)$, studied by the method of conditioning pre-

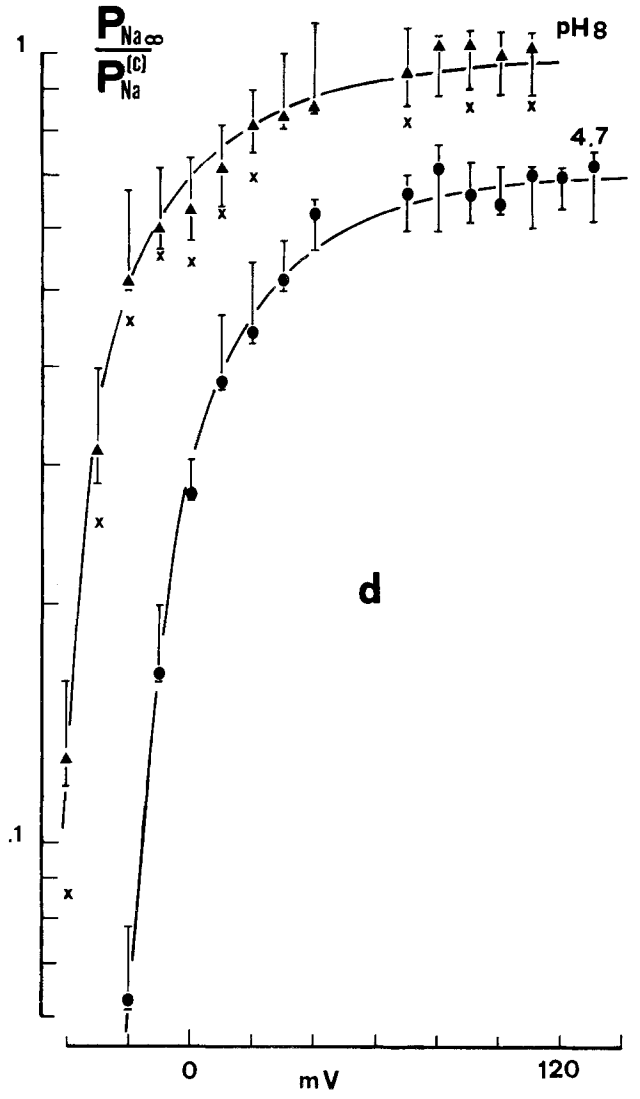

Fig. 3d

pulses (Hodgkin & Huxley, 1952*b*). The relative magnitude of peak sodium current measured during the test pulse was corrected for the leakage current and plotted against the prepulse potential. Similar results were obtained at pH 9 and 4.9.

The figure indicates the holding potential value to be used at various pH in order to satisfy the initial condition: $h_\infty(E_h)=1$. Thus, a good choice would be -80 mV ($h_\infty=0.97$) for axons in normal ASW, and -90 or -60 mV for axons in ASW at basic or acid pH. From the figure

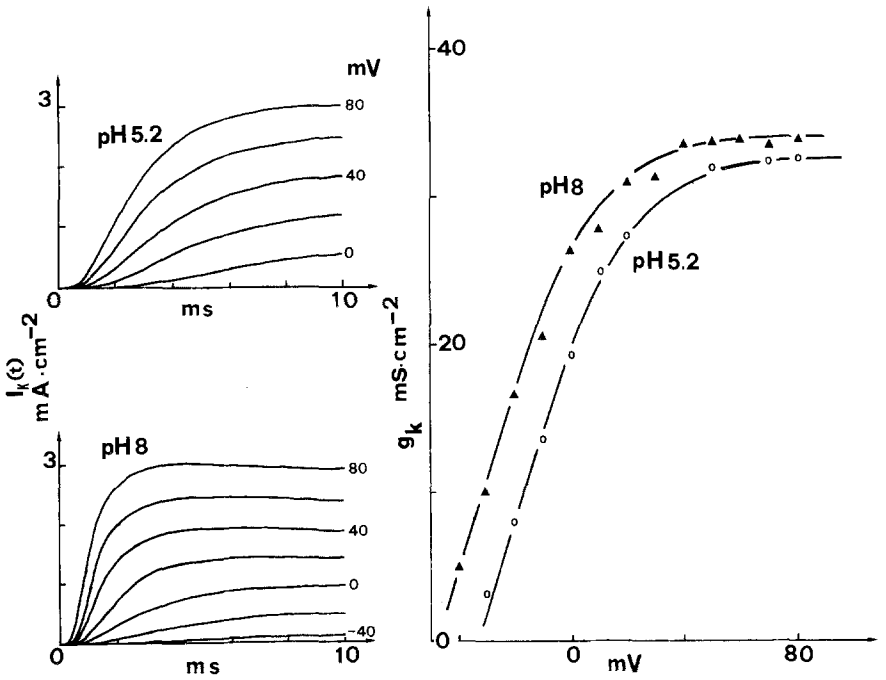

Fig. 4. Influence of external pH on potassium current, I_K (left), and instantaneous conductance, $g_{K'}$ (right). The axon was bathed in ASW + 3×10^{-7} M TTX. Depolarizing pulses lasted 20 msec at pH 8 and 45 msec at pH 5.2. Potential values in mV is given on the right of each record. Leakage and capacitative currents are subtracted. Lines were drawn by eye. $E_h = -80$ mV (pH 8), and $E_h = -70$ mV (pH 5.2). Temperature, 2 °C

we notice that the h_∞ value at -40 mV (pH 8) and -30 mV (pH 4.7) is not zero. Nevertheless, a reliable fit of membrane currents, following the standard procedure, could be obtained only assuming $h_\infty(E) = 0$ at these final potentials. This discrepancy between h_∞ measurements with the two different techniques is a rather important observation which, however, cannot be discussed in the present work, since it requires further investigations (*see* Goldman & Schauf, 1973; Goldman, 1976).

Effects of Extracellular pH on Sodium Conductance Parameters

Figure 6 shows the results of the computer analysis of membrane currents in experiments performed on different axons at various pH. The thick continuous curves represent the best fit for the control experiments. The thin lines joining the dots represent the results of the fit at low and high pH. At low pH the different parameters are shifted by different

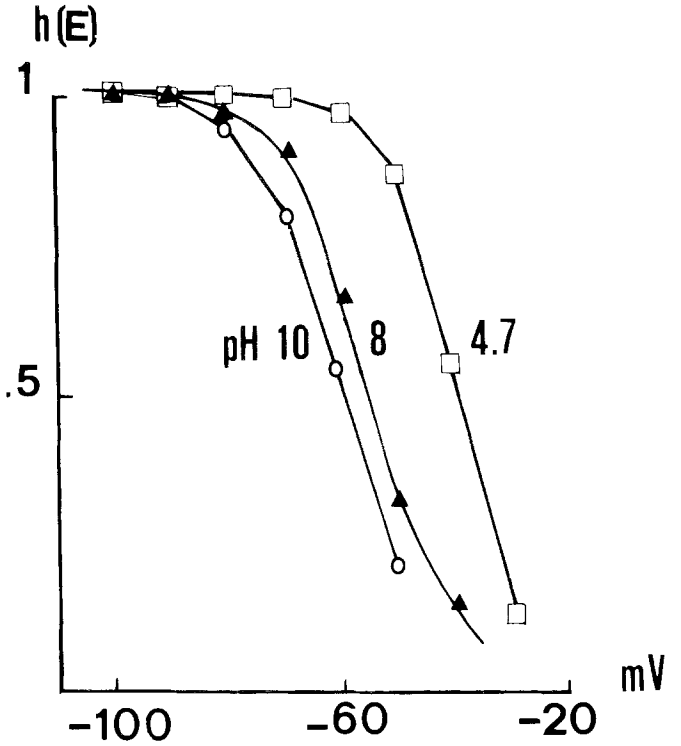

Fig. 5. Steady-state inactivation curve at basic and acid pH. *Ordinate:* normalized peak sodium current. *Abscissa:* membrane potential during conditioning prepulse. Conditioning steps lasted 200 msec; 0.8 msec test pulse to 0 mV, $E_h = -60$ mV. Data from two different axons having similar $h(E)$ curves at pH 8 (filled triangles). Buffer solutions were: Na-borate, pH 10 (open circles), and Na-phthalate, pH 4.7 (open squares). Temperature, 2 °C

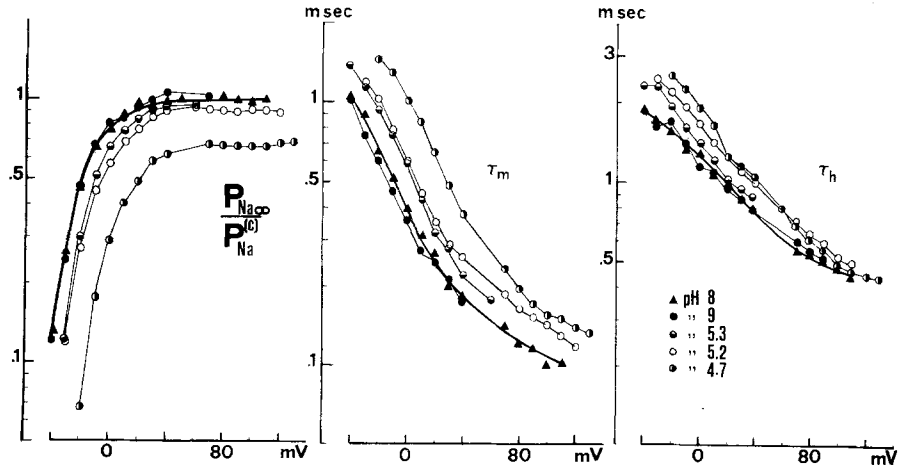

Fig. 6. Sodium conductance parameters *vs.* voltage at different external pH as obtained by fitting the current records according to the method described in Data Analysis. Smooth thick lines and filled triangles represent the average from seven axons at pH 8. Temperature, 1.8–3 °C

amounts along the voltage axis. In the range examined, lowering the pH produced a depression of the maximum permeability, $\bar{P}_{Na}$, which never exceeded 25%.

In order to test the goodness of our fit, we compared the data of Fig. 6 with the peak sodium permeability values obtained from the same axons at pH 5.2 and 4.7 (*see* Fig. 3). This could be done by converting the peak permeabilities of Fig. 3*a–b* into steady-state quantities according to the following equation:

$$P_{Na_p} = (3\omega/(1+3\omega))^3 \cdot (1/(1+3\omega))^{1/\omega} \cdot P_{Na_\infty}, \tag{4}$$

where $\omega = \tau_h/\tau_m$ and $P_{Na_\infty} = m_\infty^3 \bar{P}_{Na}$ is the hypothetical steady-state value that would be reached if the effects of the exponentially developing inactivation were removed. Eq. (4) accounts for changes in the kinetics parameters and is derived from Eq. (19) of Hodgkin and Huxley (1952*c*) at the time of peak, t_p, after substitution of the value: $t_p = \tau_m(1+\ln\omega)$, calculated from the condition: $\delta P_{Na}/\delta t = 0$ (Conti *et al.*, 1973).

The results obtained by the two methods are summarized in Fig. 3*c–d*. The triangles (pH 8) and circles (pH 5.2 and 4.7) represent the normalized P_{Na_∞} values calculated from the data of Fig. 3*a–b* according to Eq. (4). The ratios τ_h/τ_m were obtained directly from Fig. 6. All the points are seen to fall within the error bars which indicate the upper and lower limit of the $P_{Na_\infty}/\bar{P}_{Na}$ values obtained from the fit. The continuous lines fitting the triangles were drawn by eye, while those below are the same curves lowered and displaced sidewise to match the circles. Apart from other considerations, the agreement between the two types of approaches gives confidence in the validity of the curve-fitting method and allows a correct estimate of the voltage shift and amplitude depression of the maximum sodium permeability.

Effects on Activation and Inactivation Rate Constants

The rate constants α_m and β_m of the activation process are calculated directly from the data of Fig. 6 and plotted against voltage in Fig. 7*a–b*. In acidic solutions $\alpha_m(E)$ is displaced toward more depolarized voltages, while $\beta_m(E)$ is barely affected. This would suggest that the opening and closing rate constants are differently influenced by the electric field which is generated by the fixed negative charges at the external and internal membrane surfaces (Chandler, Hodgkin & Meves, 1965).

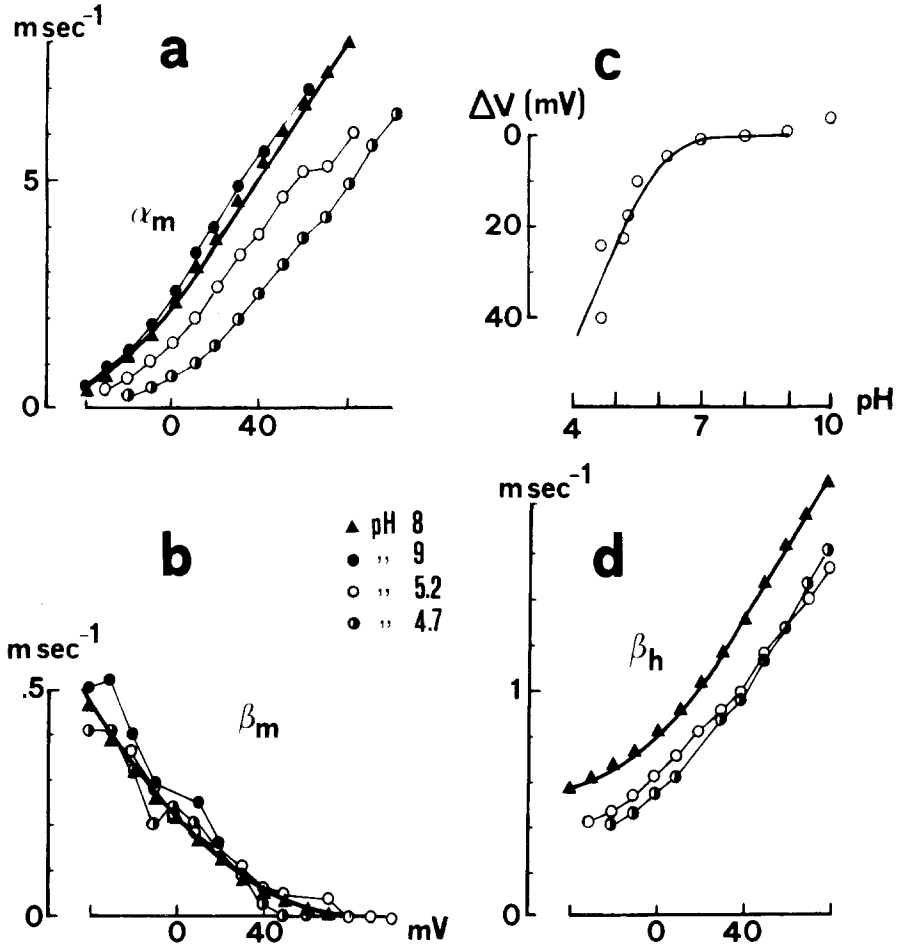

Fig. 7. (*a*)–(*b*): Rate constants of sodium activation (α_m and β_m) as function of membrane potential. Thick lines and dots are calculated from Fig. 6. Symbols correspond to those of Fig. 6. (*c*): pH dependence of sodium activation kinetics. Open circles represent the displacement of α_m along the voltage axis (ΔV) measured with respect to normal pH. ΔV values are taken at large depolarizing voltages where the curves are approximated by parallel straight lines. The smooth curve is the result of a theoretical fit based on a fixed surface charge model (*see* text). (*d*): Rate constant β_h of activation *vs.* membrane potential. The lines are obtained by inverting the data of Fig. 6

A plot of the voltage shifts of $\alpha_m(E)$ as a function of pH is shown in Fig. 7*c*. Each point is taken from a different axon. The continuous curve illustrates the result of a theoretical fit carried out according to the fixed surface charges model described by Gilbert and Ehrenstein (1969) using the following values of parameters: $\sigma_t = 1.6 \times 10^{-2}$ electronic charges· $Å^{-2}$ (which corresponds to an average charge separation of 8 Å), $K = 30\,mM^{-1}$ and $B = -62$ mV. The value $30\,mM^{-1}$ for the equilibrium

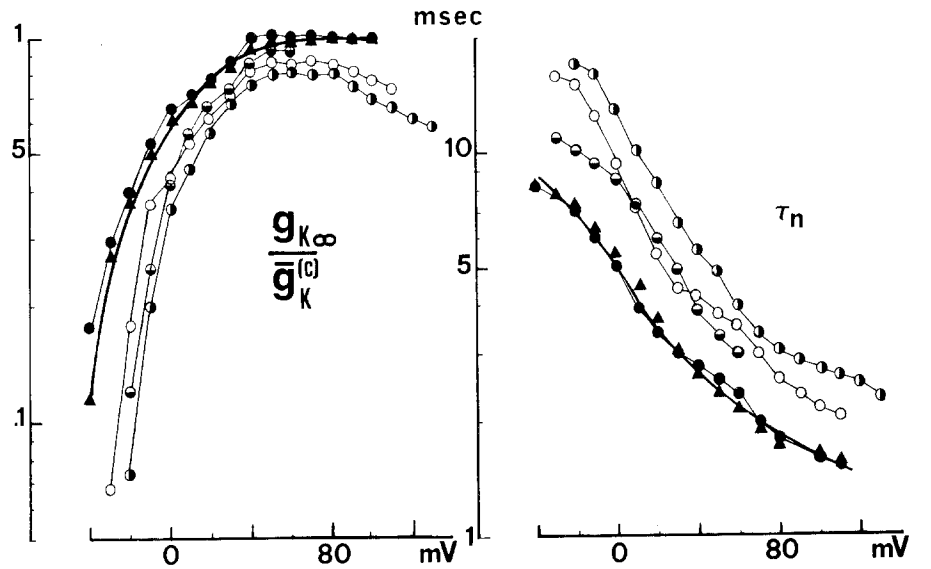

Fig. 8. Voltage dependence of potassium conductance parameters as obtained from the fit at different external pH. Data are corrected from the "K^+ ion accumulation" according to the procedure described in *Materials and Methods*. Thick and thin lines have the same meaning as in Figs. 6 and 7. *Left:* potassium conductance g_{K_∞} *vs.* voltage, normalized to the maximum conductance $\bar{g}_K^{(c)}$ at pH 8. *Right:* the time constant of potassium conductance τ_n *vs.* membrane potential

constant corresponds to a pK_a of 4.5, close enough to the pK_a values of carboxylic acid groups.

The model proposed by Gilbert and Ehrenstein is based on the assumption that negative fixed charges on the external membrane surface can be neutralized by the addition of a titrating ion such as H^+, according to a first order chemical reaction. Under these conditions, the diffuse double layer potential, $V = V_{1/2} - B$, and the maximum surface charge density, σ_t, at the external surface of the axon are related by the expression (Gilbert & Ehrenstein, 1970):

$$\sigma_t \cdot [1 + K[H]_0 e^{F(B-V_{1/2})/RT}]^{-1} = C \cdot \left\{ \sum_{i=1}^{m} c_i [e^{z_i F(B-V_{1/2})/RT} - 1] \right\}^{-1/2}, \qquad (5)$$

where K is the intrinsic equilibrium constant regulating the screening of negative charges by protons; $[H]_0$ is the concentration of hydrogen ions in bulk solution; m is the number of ionic species; c_i and z_i are, respectively, the ion concentration in bulk solution and the valence of ionic species i; $V_{1/2}$ is the electrical potential at the midpoint of the $\alpha_m(E)$ curve; B is an arbitrary constant determining reference for potential shifts and C is a constant at a given temperature.

Finally, the effects of external pH on β_h are illustrated in Fig. 7*d*. The data are the inverse of the τ_h values in Fig. 6, since for $E > -40$ mV $h_\infty(E)$ was assumed to be zero. As can be seen, β_h behaves similarly to α_m, but the shift for pH 4.7 is much less pronounced. Also, β_h barely recovers

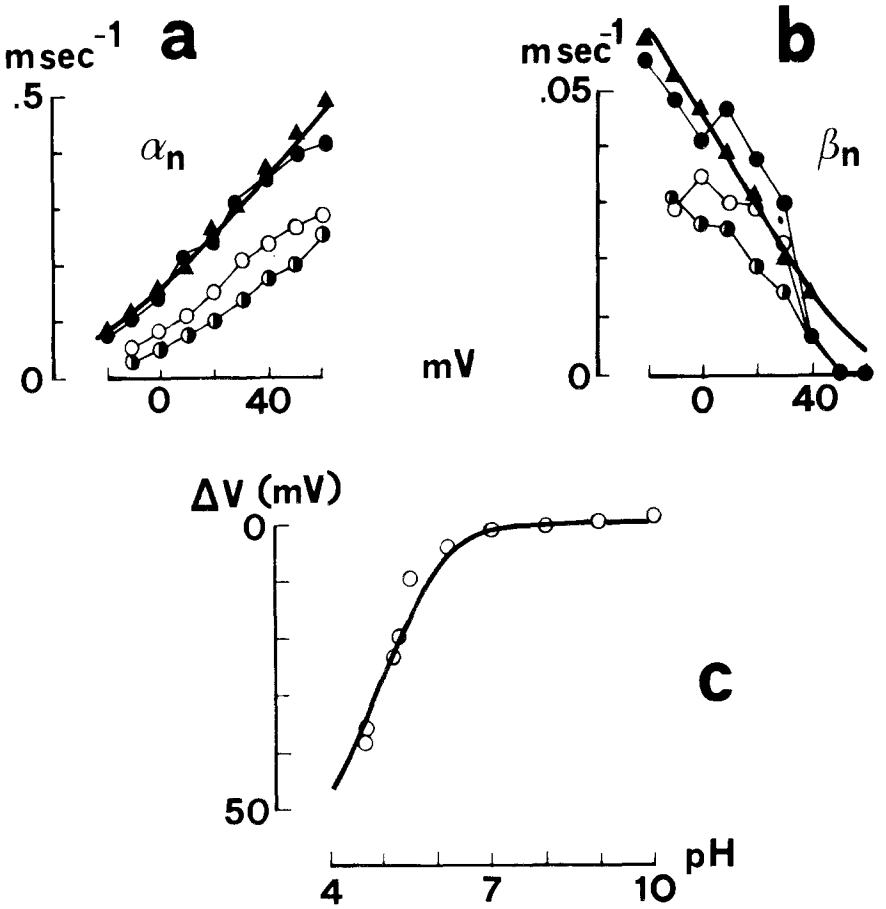

Fig. 9. Voltage dependence of rate constants α_n (*a*) and β_n (*b*) of potassium kinetics and voltage-shift (*c*), ΔV, of $\alpha_n(E)$ as a function of external pH. Discontinuous lines are obtained from Fig. 8. Open circles in (*c*) represent displacements of α_n with respect to normal pH, along the voltage axis. ΔV values are taken at large depolarizing voltages where $\alpha_n(E)$ can be approximated by parallel straight lines. The smooth curve is the result of a theoretical fit (*see* text)

after acidic treatments below pH 6, while α_m and β_m have an almost complete reversibility down to pH 4.7. The conclusion suggested by these results is that activation and inactivation processes are affected differently by changing the external pH.

Effects of Extracellular pH on Steady State and Rate of Rise of Potassium Conductance

The action of external pH on the parameters describing the potassium conductance is shown in Fig. 8. Similar to the sodium con-

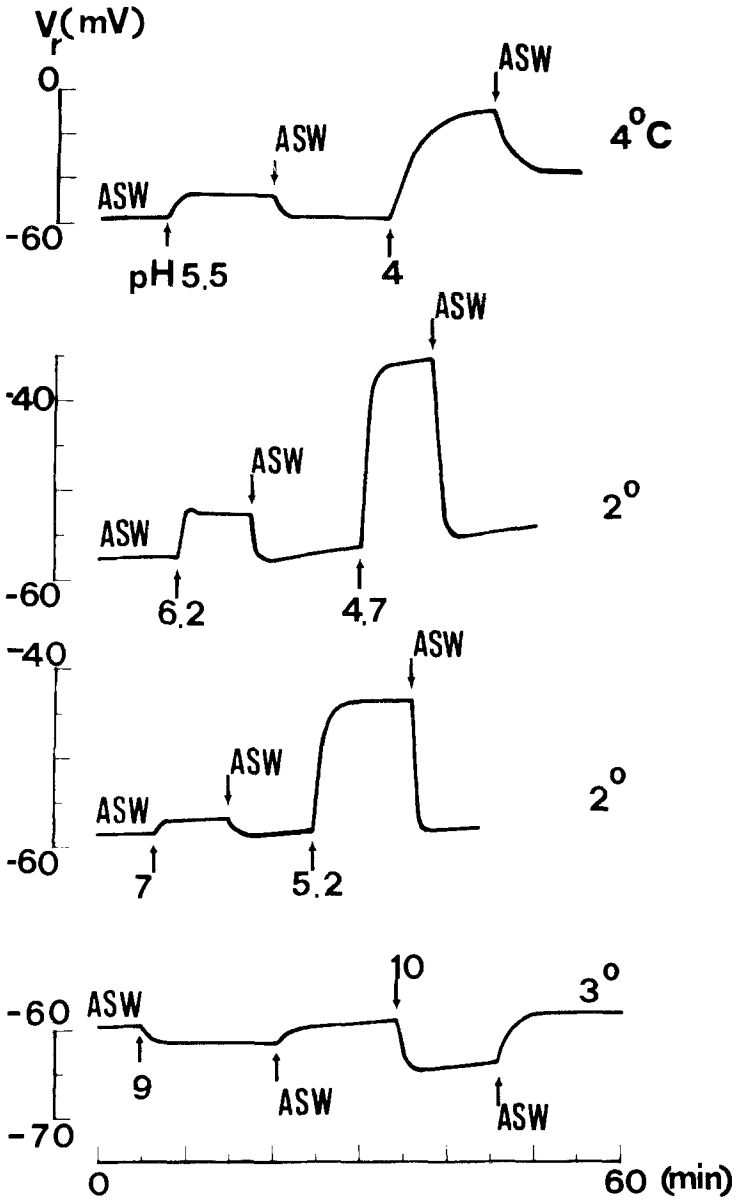

Fig. 10. Time course of resting membrane potential during pH changes. *Ordinate:* membrane resting potential in mV. *Abscissa:* time after impalement of fiber. All records start from normal external solution at pH 8. Arrows indicate instant when the exchanged solution starts acting. Note different scale on top trace

ductance, the steady-state value, $g_K(E)$, and the time constant, $\tau_n(E)$, are influenced differently by changes in extracellular pH. Increasing the acidity, the normalized steady-state conductance curves are depressed and displaced toward more positive potentials. In particular, the slight

depression at potentials between 60 and 80 mV is followed at large depolarizations by a consistent fall. We attribute this last effect to a block of the potassium channel by internal sodium ions (Bezanilla & Armstrong, 1972) because the magnitude of the depression increased progressively with time; axons having a low E_{Na}, i.e., a large Na content, showed more pronounced effects. Under these conditions we found it very difficult to ascertain whether the 10–20% $\bar{g}_K$ reduction measured at 80 mV, could be attributed to a block by external hydrogen ions or by internal monovalent cations.

The effects of external pH on $\tau_n(E)$ are similar to those described for $\tau_m(E)$. A plot of the rate constants α_n and β_n as a function of voltage shows that $\alpha_n(E)$ undergoes a shift similar to $\alpha_m(E)$ upon changing the pH, while $\beta_n(E)$ behaves differently (Fig. 9). Indeed, $\beta_n(E)$ is seen to shift in the opposite direction, toward more hyperpolarizing potentials as the pH is decreased. This observation is supported by the results of experiments carried out on TTX-treated axons in which the displacements were found to be consistent with those reported in Fig. 9*a–b*.

Figure 9*c* shows the voltage shift of $\alpha_n(E)$ as a function of external pH. Data are taken from different axons while the continuous curve is obtained following the procedure mentioned above. The corresponding values of the parameters are: average charge separation, 7.3 Å; equilibrium constant, 30 mM^{-1}, and external surface potential, −67 mV.

The effects of changing the external pH on the resting potential were also investigated. The results obtained from four different axons are illustrated in Fig. 10. External acidic solutions are seen to depolarize the membrane. The resting potential variations are roughly proportional to the external pH change. Recovery is always within 80% of the initial value except for the experiment at pH 4. This feature was consistently observed each time the nerve was treated with external solutions having pH below 4.7.

Discussion

Rate Constants of Sodium and Potassium

Most of the results reported in this paper can be summarized by saying that changes in the external H^+ concentration alter the electrostatic potential energy profile of specific membrane components responsible for the control of sodium and potassium permeability.

Our study shows that the different shifts observed for $P_{Na_\infty}(E)/\bar{P}_{Na}$ and $\tau_m(E)$ (or $g_{K_\infty}(E)/\bar{g}_K$, $\tau_n(E)$) originate from a distinct pH dependence of the opening and closing rate constants α and β. $\alpha_m(E)$ and $\beta_m(E)$ (or α_n(E),

$\beta_n(E)$) are displaced differently along the potential axis by changing the pH of extracellular bath. Shrager (1974) suggested that the partial neutralization of a negative surface potential produced by lowering the pH cannot account for these asymmetrical voltage dependencies, concluding that the absence of $\beta_n(E)$ displacements might depend on a chemical alteration of the energy profile of both potassium gating components. This model qualitatively fits our data. It predicts that β_n would not increase proportionally to the decrease of α_n, and that in some cases β_n might even decrease as the external pH is lowered. However, the model is not suitable for explaining the pH dependence of α_n at various depolarizations. In other words, it cannot account for the fact that the ratio of α_n at low and normal pH changes with the potential, implying that for the same preparation one obtains curves of α_n versus pH of different shapes, depending on the potential value considered.

At this stage of knowledge, a general description of the conditions required to meet the present data seems more reasonable than proposing alternative models. In this respect, rate constants α and β can be thought as being distinct functions of the voltage across the membrane, controlled by molecular components with potential energy profiles affected differently by the titrating action of hydrogen ions. Thus, the fit of the voltage shift of $\alpha_m(E)$ versus pH, shown in Fig. 8*c*, would suggest that α_m is influenced by the field generated by unspecific negatively charged groups with a local density around the Na^+ channel of one electron charge every 64 $Å^2$ and having a pK of 4.5. Similar figures are obtained for α_n. This interpretation, based on a restricted number of experiments, is clearly too speculative to be expanded at present.

Maximum Sodium and Potassium Conductance

In the range examined, external pH has only a small influence on the maximum sodium permeability, $\bar{P}_{Na}$. Above pH 5 $\bar{P}_{Na}$ is within 10% of the value at normal pH, while at pH 4.7 $\bar{P}_{Na}$ decreased by 25%. Below pH 4.7 the fibers undergo irreversible changes, which make it difficult to quantify the degree of the depression.

Our results agree with those of Stillman *et al.* (1971) and Gilbert, Stillman & Lipicky (1972), who found that maximum sodium currents decrease while the time to reach peak increases as the pH of the bath was lowered. Previous work on other preparations also shows that peak sodium permeability decreases at acid pH with approximate pK_a's of 5.2 (Hille, 1968) and 4.5 (Drouin & Neumcke, 1974) in frog nodes and 4.8 in

Myxicola axons (Schauf & Davis, 1976). The voltage-dependent block of Na^+ channel observed by Woodhull (1973) (50% at $E = +100$ mV) in frog node also seems to be present in our preparation when measuring peak sodium permeabilities at very low pH (*see* in Fig. 3*b* the continuing, gradual increase of P_{Na} for $E > 40$ mV). However, this phenomenon can barely be detected in the corresponding Fig. 3*d* once the peak permeabilities are converted into steady-state quantities, suggesting that in squid the block of Na^+ channel is nearly independent of the voltage applied across the membrane. Anyway, this fact does not prevent qualitative comparison of our Fig. 3 results with those reported by Woodhull. If we do so, we can conclude that external protons act more effectively in frog nodes than in squid axons.

The effects of pH on maximum potassium conductance agree qualitatively with those reported by Shrager (1974) on crayfish axons. They also coincide with the observations of Stillman *et al.* (1971) in squid, reporting little influence of pH on the magnitude of potassium currents until pH dropped below 5. In the frog node Hille (1973) reported a voltage-dependent block of potassium channels attributable (at high depolarizing voltages) to the tritation of a single acid group with a pK_a of 4.4. Schauf and Davis (1976) also found a $\bar{g}_K$ depression in *Myxicola* giant axons consistent with the titration of a weak acid having similar pK_a. Again, a direct comparison of the data seems difficult. The presence of K^+ ion accumulation (Frankenhaeuser & Hodgkin, 1956) on different nerve preparations and the effects of internal Na ions (Bezanilla & Armstrong, 1972), if not correctly taken into account, might influence the $\bar{g}_K$ measurements, leading to substantially different results.

One might suspect that the depression of maximum sodium and potassium permeability and the voltage shift of the rate constants, associated with extracellular pH changes, is induced by a variation of intracellular pH. Since there is evidence that in squid axons the internal pH changes with the external (Spyropoulos, 1960; Bicher & Ohki, 1972) and that the internal pH is much more critical than the external (Tasaki, Watanabe & Takenaka, 1962), this possibility cannot be excluded *a priori*, and one must be careful in drawing general conclusions from the data reported here. Studies similar to those presented above, performed under controlled internal pH, would be important for a complete understanding of the phenomena under study.

We would like to thank Dr. F. Conti for helpful discussions and a critical reading of the manuscript. The comments of Dr. B. Neumcke on a preliminary version of the paper are also gratefully acknowledged.

References

Adams, G. 1973. The effect of potassium diffusion through the Schwann cell layer on potassium conductance of the squid axon. *J. Membrane Biol.* **13**:353

Adelman, W.J., Jr., Palti, Y., Senft, J.P. 1973. Potassium ion accumulation in a periaxonal space and its effect on the measurement of membrane potassium ion conductance. *J. Membrane Biol.* **13**:387

Bezanilla, F., Armstrong, C.M. 1972. Negative conductance caused by entry of sodium and cesium ions into the potassium channels of squid axons. *J. Gen. Physiol.* **60**:588

Bicher, H.I., Ohki, S. 1972. Intracellular pH electrode experiments on the giant squid axon. *Biochim. Biophys. Acta* **255**:900

Caldwell, P.C. 1958. Studies on the internal pH of large muscle and nerve fibers. *J. Physiol. (London)* **142**:22

Chandler, W.K., Hodgkin, A.L., Meves, H. 1965. The effect of changing the internal solution on sodium inactivation and related phenomena in giant axons. *J. Physiol. (London)* **180**:821

Chandler, W.K., Meves, H. 1965. Voltage clamp experiments on internally perfused giant axons. *J. Physiol. (London)* **180**:788

Cole, K.S., Moore, J.W. 1960. Liquid junction and membrane potentials of the squid giant axon. *J. Gen. Physiol.* **43**:971

Conti, F., De Felice, L.J., Wanke, E. 1975. Potassium and sodium ions current noise in the membrane of the squid giant axon. *J. Physiol. (London)* **248**:45

Conti, F., Fioravanti, R., Wanke, E. 1973. Caratteristiche elettriche dello stato attivo dei siti del sodio nella membrana nervosa. 1st *Ital. Bioph. Soc. Meet.* **1**:413

Conti, F., Wanke, E. 1975. Channel noise in nerve membranes and lipid bilayers. *Q. Rev. Biophys.* **8**:451

Dodge, F.A., Frankenhaeuser, B. 1959. Sodium currents in the myelinated nerve fibre of *Xenopus laevis* investigated with the voltage clamp technique. *J. Physiol. (London)* **148**:188

Drouin, H., Neumcke, B. 1974. Specific and unspecific charges at the sodium channels of the nerve membrane. *Pfluegers Arch.* **351**:207

Ehrenstein, G., Fishman, H.M. 1971. Evidence against hydrogen-calcium competition model for activation of electrically excitable membranes. *Nature New Biol.* **233**:16

Frankenhaeuser, B., Hodgkin, A.L. 1956. The after-effects of impulses in the giant nerve fibres of *Loligo*. *J. Physiol. (London)* **131**:341

Gilbert, D.L., Ehrenstein, G. 1969. Effect of divalent cations on potassium conductance of squid axons. Determination of surface charge. *Biophys. J.* **9**:447

Gilbert, D.L., Ehrenstein, G. 1970. Use of a fixed charge model to determine the pK of the negative sites on the external membrane surface. *J. Gen. Physiol.* **55**:822

Gilbert, D.L., Stillman, J.M., Lipicky, R.J. 1972. Effect of external pH on the sodium current, in the squid giant axon. *IV. Int. Biophys. Congr. Abstr. (Moscow)* **3**:227

Goldman, D.E. 1943. Potential, impendance and rectification in membranes. *J. Gen. Physiol.* **27**:37

Goldman, L. 1976. Kinetics of channel gating in excitable membranes. *Q. Rev. Biophys.* **9**:491

Goldman, L., Schauf, C.L. 1973. Quantitative description of sodium and potassium currents and computed action potentials in *Myxicola* giant axons. *J. Gen. Physiol.* **61**:361

Hille, B. 1968. Charges and potentials at the nerve surface. Divalent ions and pH. *J. Gen. Physiol.* **51**:221

Hille, B. 1973. Potassium channels in myelinated nerve. Selective permeability to small cations. *J. Gen. Physiol.* **61**:669

Hodgkin, A.L., Huxley, A.F. 1952*a*. Current carried by sodium and potassium ions through the membrane of the giant axon of *Loligo*. *J. Physiol. (London)* **116**:449

Hodgkin, A.L., Huxley, A.F. 1952*b*. The dual effect of membrane potential on sodium conductance in the giant axon of *Loligo*. *J. Physiol. (London)* **116**:497

Hodgkin, A.L., Huxley, A.F. 1952*c*. A quantitative description of membrane current and its application to conduction and excitation in nerve. *J. Physiol. (London)* **117**:500

Hodgkin, A.L., Katz, B. 1949. The effect of sodium ions on the electrical activity of the giant axon of the squid. *J. Physiol. (London)* **108**:37

Keynes, R.D., Rojas, E. 1976. The temporal and steady-state relationships between activation of the sodium conductance and movement of the gating particles in the squid giant axon. *J. Physiol. (London)* **255**:157

Mozhayeva, G.N., Naumov, A.P. 1970. Effect of surface charge on the steady-state potassium conductance of nodal membrane. *Nature (London)* **228**:164

Schauf, C.L., Davis, F.A. 1976. Sensitivity of the sodium and potassium channels of *Myxicola* giant axons to changes in external pH. *J. Gen. Physiol.* **67**:185

Shrager, P. 1974. Ionic conductance changes in voltage clamped crayfish axons at low pH. *J. Gen. Physiol.* **64**:666

Spyropoulos, C.S. 1960. Cytoplasmic pH of nerve fibers. *J. Neurochem.* **5**:185

Stillman, J.M., Gilbert, D.L., Lipicky, R.J. 1971. Effect of external pH upon the voltage-dependent currents of the squid giant axon. *Biophys. Soc. Ann. Meet. Abstr.* **11**:55*a*

Tasaki, I., Watanabe, A., Takenaka, T. 1962. Resting and action potential of intracellularly perfused squid giant axon. *Proc. Nat. Acad. Sci. USA* **48**:1177

Woodhull, A.M. 1973. Ionic blockage of sodium channels in nerve. *J. Gen. Physiol.* **61**:687